A Rehabilitation Robot With Force-Position Hybrid Fuzzy Controller: Hybrid Fuzzy Control of Rehabilitation Robot

Article *in* IEEE Transactions on Neural Systems and Rehabilitation Engineering · October 2005

DOI: 10.1109/TNSRE.2005.847354 · Source: PubMed

5 authors, including:

Ming-Shaung Ju
National Cheng Kung University

Chou-Ching K Lin
National Cheng Kung University

Ing-Shiou Hwang
National Cheng Kung University

A Rehabilitation Robot With Force-Position Hybrid Fuzzy Controller: Hybrid Fuzzy Control of Rehabilitation Robot

Ming-Shaung Ju, Chou-Ching K. Lin, Dong-Huang Lin, Ing-Shiou Hwang, and Shu-Min Chen

***Abstract*—The goal of this study was to design a robot system for assisting in the rehabilitation of patients with neuromuscular disorders by performing various facilitation movements. The robot should be able to guide patient's wrist to move along planned linear or circular trajectories. A hybrid position/force controller incorporating fuzzy logic was developed to constrain the movement in the desired direction and to maintain a constant force along the moving direction. The controller was stable in the application range of movements and forces. Offline analyses of data were used to quantitatively assess the progress of rehabilitation. The results show that the robot could guide the upper limbs of subjects in linear and circular movements under predefined external force levels and apply a desired force along the tangential direction of the movements.**

***Index Terms*—Fuzzy control, hybrid position/force control, rehabilitation robot.**

I. Introduction

REHABILITATION program is the main stay of treatment for patients suffering from trauma, stroke, or spinal cord injury. Conventionally, these programs rely heavily on the experience and manual manipulation of the therapists. Since the number of patients is large and the treatment is time consuming, it is a big advance if robots can assist in performing treatment. Noritsugu *et al.* [1] designed an arm-like robot for treating patients with trauma, and developed four modes of linear motion with impedance control to control the force during the movement. They used adaptive identification method to estimate the stiffness of the affected limb as an indicator of recovery. Krebs *et al.* [2] designed a planar robot with impedance control for guiding patients to make movements along the specified trajectories. These trajectories had different stimulatory effects on elbow and shoulder joints. They showed beneficial effects of the robot with qualitative evaluation scales. Ju *et al.* [3] added different constant external loads, by a robot in torque control mode, to the elbow while the stroke patients were performing voluntary tracking of constant velocity movements of their elbow. The results indicated that both assistive and resistive loads improved the voluntary performance. Cozens [4], using a single axis robot and torque control mode, applied resistive or assistive torque to the elbow for rehabilitation of patients with spasticity and weakness. They measured electromyographic signals of biceps and triceps as an indicator of reciprocal activation and concluded that the externally imposed forces had beneficial effects. Reinkensmeyer *et al.* [5] showed that a counterpoise assistive controller that compensated for gravity and elbow passive properties could partially improve reaching movements in patients with brain injuries.

One of the major difficulties in realizing rehabilitation by robots is the controller design. Simple linear movement with simple velocity profile is relatively easy to design. Yet, manual treatments usually involve complex maneuvers with resistive or assistive force imposed at specific points of the movement. Circular or more complex movements with predefined imposing force are difficult to design. While conventional position controllers control position, not force, conventional force controllers regulate force without precise control of the movement trajectory. Another is the isotropic control or impedance control that maintains a constant endpoint stiffness and damping. Hybrid position/force controllers [6], [7], controlling position in one direction and force in the orthogonal direction, have the advantage of simultaneously maintaining the desired movement trajectory and force for the planar movements. An alternative approach was adopted in the active-constrained mode of mirror image movement enabler (MIME) system [8], [9]. The robot provided a viscous resistance in the direction of desired movement and spring-like forces in all other directions. Thus, the system had position control in one direction and velocity-dependent force control in the other direction. The reaching guide developed by Reinkensmeyer *et al.* [5], in a general sense, also implemented position control in one direction and force control in the other direction. Yet, the position control was provided by the hardware constraint. One additional problem in designing the controller is the uncertainty about the subject and the nonlinear dynamics of the robot such as the Coulomb friction in the mechanism. In a classical design process, the control parameters are determined according to the system model and its parameters. For a rehabilitation program assisted by a robot, the subject is also part of the dynamic system and the dynamics model of the subject is not as clear and invariable as the mechanical system. To solve this problem, fuzzy

Manuscript received January 9, 2003; revised August 17, 2003 and August 25, 2004; accepted: December 28, 2004. This work was supported in part by the Republic of China National Science Council under Contract NSC 89-214-B-006–057 and Contract NSC 87-2314-B-006-125-M08.

M.-S. Ju and D.-H. Lin are with the Department of Mechanical Engineering, National Cheng Kung University, Tainan 70101, Taiwan, R.O.C. (e-mail: msju@mail.ncku.edu.tw).

C.-C. K. Lin is with the Department of Neurology, National Cheng Kung University Hospital, Tainan 70101, Taiwan, R.O.C.

I.-S. Hwang is with the Department of Rehabilitation, National Cheng Kung University Hospital, Tainan 70101, Taiwan, R.O.C.

S.-M. Chen is with the Department of Physical Therapy, National Cheng Kung University Hospital, Tainan 70101, Taiwan, R.O.C.

Digital Object Identifier 10.1109/TNSRE.2005.847354

logic is incorporated in the current position and force control algorithms. Fuzzy control [10]–[12] is known for coping with nonlinear systems and systems that have uncertainty in its parameters. Yet, a main problem associated with fuzzy control is to demonstrate the global stability [13]. Many researchers have tried to maintain the stability by fine tuning or modifying a stable linear proportional, integral, and derivative (PID) controller [14]–[16]. In the past, we successfully applied fuzzy control to the above-knee prostheses and cycling exercise by functional electrical stimulation [17]–[19]. Designing a controller for rehabilitation robot is more difficult, because the external disturbance itself is subjected to another unresolved controller (the human control).

The main purpose of the current study is to construct a robotic system specialized for rehabilitation of elbow and shoulder. The robot, incorporating hybrid position/force control and fuzzy logic, shall be able to assist the subject in performing both passive and active movements along the designed trajectories with specified loads. The actual position and force data are collected simultaneously for offline analyses. The specific goals of current work include robot construction with control algorithm implementation, trajectory planning, preliminary clinical evaluation, and performance analyses with subjects.

II. Methods

A. Experimental Setup

The experimental setup consisted of a robot mechanism, motion controller, position and force–torque sensors, and a personal computer. With a wide strip attached to the robot mechanism, the upper limb of the subject was suspended at a horizontal position and the hand in pronation. The subject's wrist was attached to the force–torque transducer with a clamp that allowed free pronation/supination. An elastic wrist–hand orthosis maintained the wrist in a pronation position. A strap supported the proximal forearm with the shoulder in 90° of abduction. For the command generation, the commands calculated by the personal computer were converted into analog signals through a D/A card (PCL726, Advantech Inc., http://www.advantech.com) and sent to drivers of two ac motors of the robot. The inputs to the controller consisted of endpoint force and position information. Endpoint force was detected by a force sensor (MC3A-S1000, Advanced Mechanical Technology Inc., Watertown, MA) attached on the robot between the wrist-fixing part and Link 4 [Fig. 1(b)]. The signal from the force sensor, amplified by a custom made amplifier, was digitized by an A/D board (PCL818HD, Advantech Inc., http://www.advantech.com). The rotation of each alternating current (ac) motor was detected by an encoder attached to the motor and counted by using a counter board (PCL833, Advantech Inc., http://www.advantech.com). From the joint angles of the robot, one can calculate Cartesian coordinates of the end effector. The force and position data were used both for closed-loop control and for later offline analyses.

As shown in Fig. 1(b), we adopted the five-bar-link drive mechanism [20] for constructing the robot. The motors were located at the base (origin of X–Y coordinate system), in order to minimize the inertial loading of the whole robot system. The

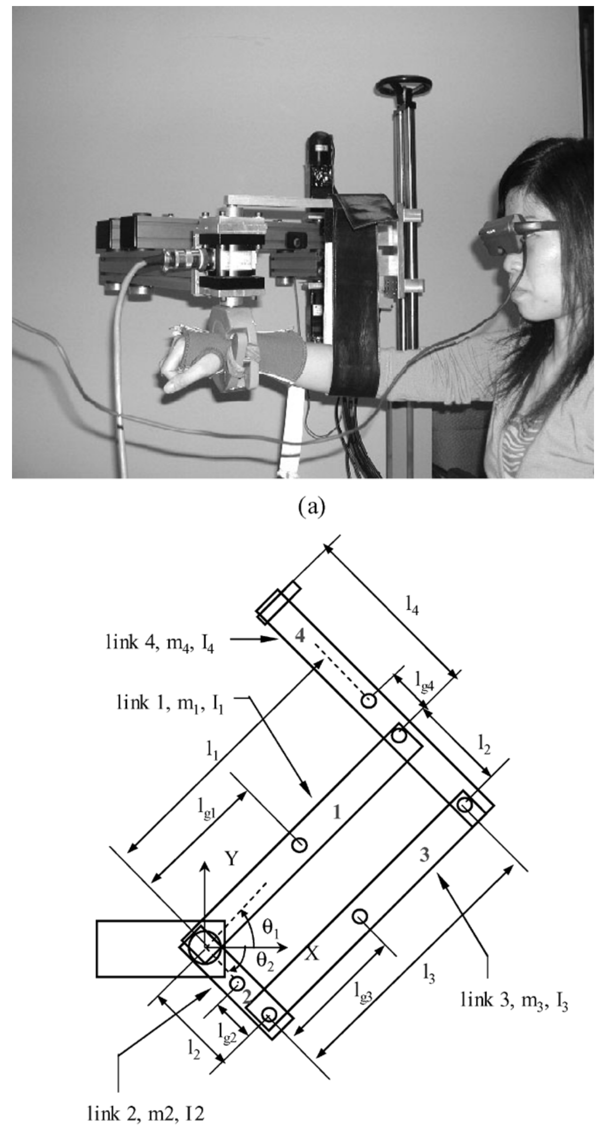

Fig. 1. Photograph of the robot-aided rehabilitation system with (a) a subject and (b) a schematic drawing of robot mechanism.

main advantage of the design was that when the physical configuration of the four links satisfied the relation of (1), the dynamic equation of the robot could be theoretically decoupled as (2)

$$\frac{m_4}{m_3}\frac{l_{g4}}{l_{g3}} = \frac{l_2}{l_1} \tag{1}$$

$$\begin{bmatrix} \tau_1 \\ \tau_2 \end{bmatrix} = \begin{bmatrix} h_{11} & 0 \\ 0 & h_{22} \end{bmatrix} \begin{bmatrix} \ddot{\theta}_1 \\ \ddot{\theta}_2 \end{bmatrix} \tag{2}$$

where m_3, m_4, l_{g3} and l_{g4} were the masses and lengths to the centers of mass of third and fourth links, respectively, l_1 and l_2 were lengths of first and second links, respectively, τ_1 and τ_2 were the input torques of the robot joints, respectively, h_{11} and h_{22} were constants, and θ_1 and θ_2 were the angles of first and second links relative to the horizontal axis (X), respectively. Equation (2) meant that the two axes were independent and it made the controller design process of simpler. The mechanism was driven by two ac motors (MSM022A1,

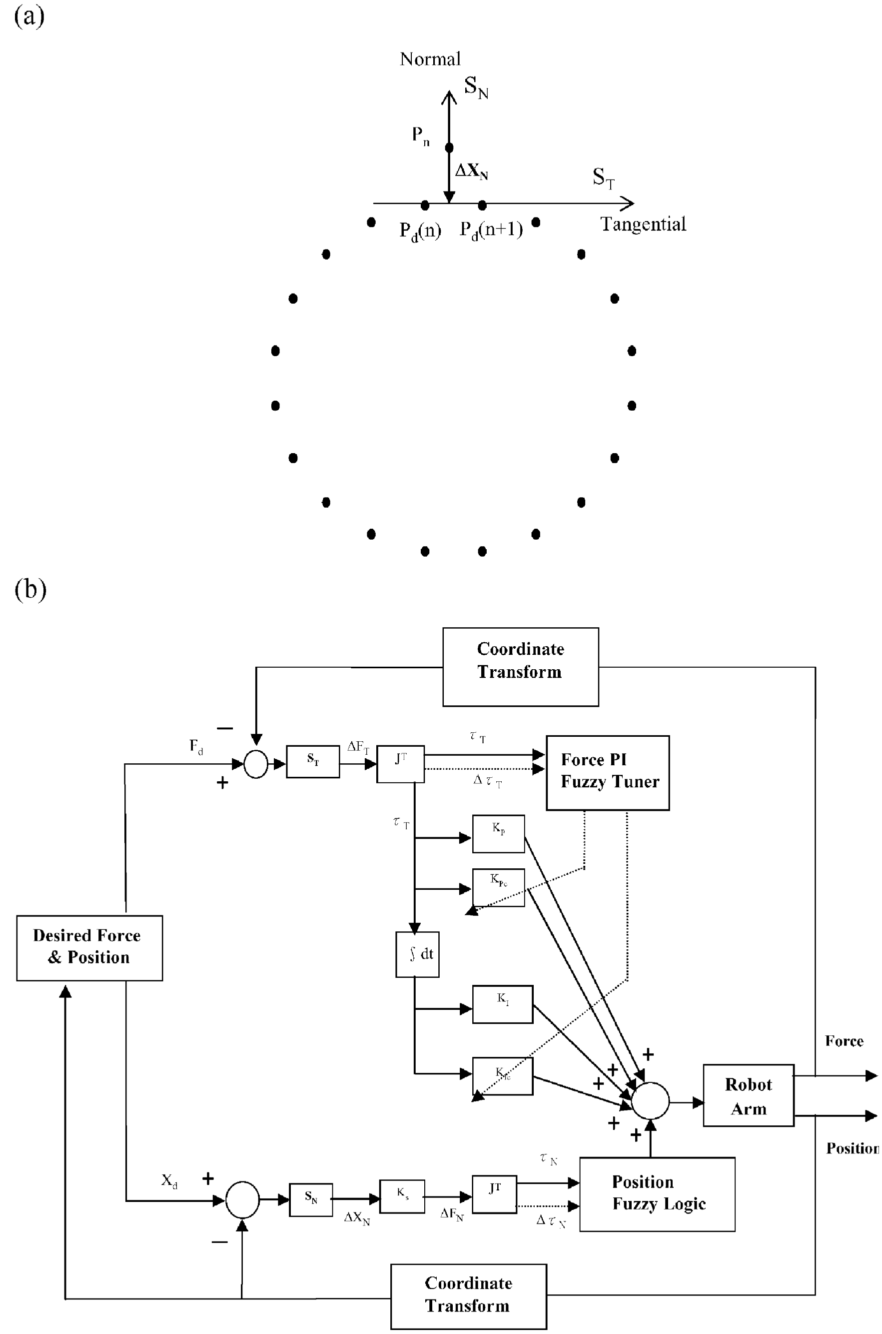

Fig. 2. (a) Definitions of the tangential direction and normal direction of movement. (b) Block diagram of the position/force hybrid control with fuzzy logics.

http://www.motionautomation.com) with a maximal torque output of 96 Nm after adding a gear speed reducer (50:1).

During the design process, we found that friction had significant effects on the robot performance and the friction torque could be added to (2), as

$$\begin{bmatrix}\tau_1\\ \tau_2\end{bmatrix} = \begin{bmatrix}h_{11} & 0\\ 0 & h_{22}\end{bmatrix}\begin{bmatrix}\ddot{\theta}_1\\ \ddot{\theta}_2\end{bmatrix} + \begin{bmatrix}\tau_{\mathrm{f1}}\\ \tau_{\mathrm{f2}}\end{bmatrix} \tag{3}$$

$$\tau_{\mathrm{fk}} = \begin{cases} b_f \cdot \dot{\theta}_k + \tau_c & \text{when } \dot{\theta}_k > 0\\ b_f \cdot \dot{\theta}_k - \tau_c & \text{when } \dot{\theta}_k < 0, \qquad k = 1, 2\end{cases} \tag{4}$$

where τ_{f1} and τ_{f2} were torques to be compensated, b_f was a constant for viscous friction term and τ_c was a static for Coulomb friction torque [21]. b_f and τ_c were determined empirically [22]. For the overall control scheme, we adopted the hybrid position/force control [6], i.e., controlling force in the tangential direction of the movement and controlling position in the orthogonal direction [Fig. 2(a)]. The main goal of control was to keep the hand of the subject in a predefined track and to impose an assistant or resistant force along the moving direction. Since force was the control goal along the moving direction, position could not be controlled and the subject could move with an individually preferred speed. In the scheme, the direction of force control ($\vec{\mathrm{S}}_{\mathrm{T}}$) was determined first by a selection matrix ($\mathbf{S_T}$) and the direction of position control ($\vec{\mathrm{S}}_{\mathrm{N}}$) was determined accordingly by another selection matrix ($\mathbf{I} - \mathbf{S_T}$), where $\mathbf{I}$ is the identity matrix. [Fig. 2(b)]

B. Position Control

Both the position and force controls were implemented in discrete time and the sampling rate was 50 Hz. The end position error along $\vec{S}_N$ was calculated first and transformed into the equivalent end force error (F_N) by a predefined stiffness constant (K_s), i.e.,

$$\Delta\vec{F}_N = K_s \cdot \Delta\vec{X}_N \tag{5}$$

where ΔX_N is the end position error along $\vec{S}_N$ in one time step. ΔF_N was transformed to the needed torque acting on joints by the Jacobian matrix (J)

$$\begin{aligned}\vec{\tau}_N &= J^T \cdot \Delta\vec{F}_N = J^T \cdot K_s \cdot \Delta\vec{X}_N,, \\ \text{where} \quad J &= \begin{bmatrix} -\mathrm{l}_1 \cdot \sin(\theta_1) & -l_4 \cdot \sin(\theta_2 + \pi) \\ l_1 \cdot \cos(\theta_1) & l_4 \cdot \cos(\theta_2 + \pi) \end{bmatrix}. \end{aligned} \tag{6}$$

τ_N and $\Delta\tau_N$ were the inputs to the fuzzy logic and were regarded as error and error change in the logic, respectively. In the fuzzification process, inputs (τ_N and $\Delta\tau_N$) were scaled and mapped to the five triangle-shaped membership functions [Fig. 3(a)], namely, large negative (LN), small negative (SN), zero (ZE), small positive (SP), and large positive (LP), respectively. One membership degree was obtained for each scaled input and membership function combination. Then, each combination of mapped inputs (E and EC) activated one control action (B_i, where i, standing for LN, SN, ZE, SP, and LP, was ith activated control function) according to the inference rule table [Fig. 3(b)]. The control rule table was determined based on the step response of a presumed second-order system, one of standard procedures for fuzzy logic control table determination [23]. We set B_i as the value at the center of base of corresponding membership function (e.g., -1 for SN) and w_i as the minimum of the membership degrees of E and EC [Fig. 3(c)]. The output of the fuzzy logic was obtained in the defuzzification process by using the center-of-gravity method

$$\tau_P = \frac{\sum_{i=1}^{n} w_i \cdot B_\mathrm{i}}{\sum_{i=1}^{n} w_i} \tag{7}$$

where τ_P was the final output of the position fuzzy controller and i indexed all the combinations of activated control actions from the rule table [Fig. 3(b)].

C. Force Control

Force control was implemented in the tangent direction of actual movement. By this convention, the robot was able to provide a desired resistive or assistive force to the subjects [24]. Since the properties of the environment (and/or the subject) were unknown *a priori*, it was impossible to determine the optimal control parameters exactly. Therefore, we combined a conventional linear PI (proportional–integral) controller and a fuzzy PI tuner as the force controller. The purpose of the fuzzy PI tuner was to compensate for the nonlinear dynamics (joint friction) of the robot and the unknown disturbing force from the subject.

(a)

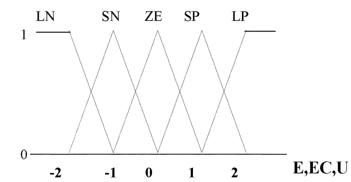

(b)

Position Control Rule

E \ EC	LN	SN	ZE	SP	LP
LN	LN	LN	LN	LN	LN
SN	LN	SN	SN	ZE	ZE
ZE	SN	SN	ZE	SP	SP
SP	ZE	ZE	SP	SP	LP
LP	LP	LP	LP	LP	LP

(c)

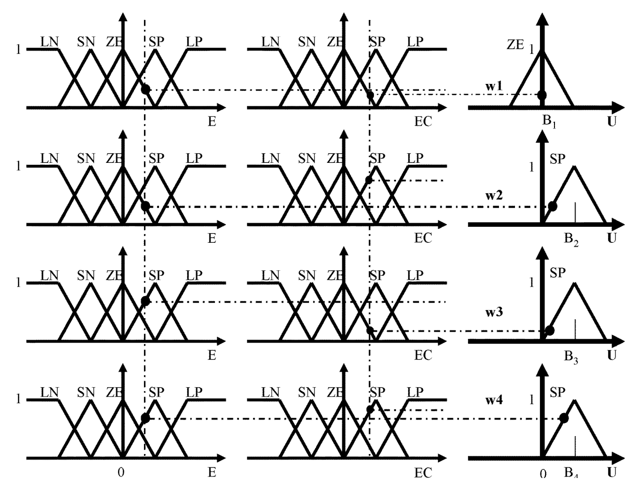

Fig. 3. (a) Membership functions and (b) the inference rule table for (c) the position controller, the fuzzy inference, or decision process. Five membership functions: LN: large negative (left thick line); SN: small negative (left dashed line); ZE: zero (solid line); SP: small positive (right dashed line); and LP: large positive (right thick line) were constructed, where E was the input. Error (τ_N) and error change ($\Delta\tau_N$) were projected to the membership function axis, respectively. Projected results (E_1 and E_2) and the corresponding membership degrees were obtained. Then, the inference rule determined B_i (the output of the fuzzification process), where $i =$ LN, SN, ZE, SP, and LP.

The force error along $\vec{S}_T$ direction (ΔF_T) was transformed into joint torque error (τ_T) by J^T. τ_T and change of it ($\Delta\tau_T$) were fed to the fuzzy PI tuner. The fuzzy PI tuner, having five membership functions in both input and output similar to the position controller described above, had separate fuzzy logics for P and I parts, and each operated in a similar way as in the position controller. The outputs from the fuzzy logic (K_{Pc} for P part and K_{Ic} for I part) were linearly combined with the conventional PI controller

$$\tau_F = \tau_T \cdot (K_P + K_{Pc}) + \int \tau_T \cdot (K_I + K_{Ic})\mathrm{dt} \tag{8}$$

where K_P and K_I were the parameters for the conventional PI controller, respectively, and τ_F was the final output of the force control. The maximal values of K_{Pc} and K_{Ic} were set to be equal to K_P and K_I, respectively.

The whole controller was realized by using C language in DOS environment in a 486 personal computer.

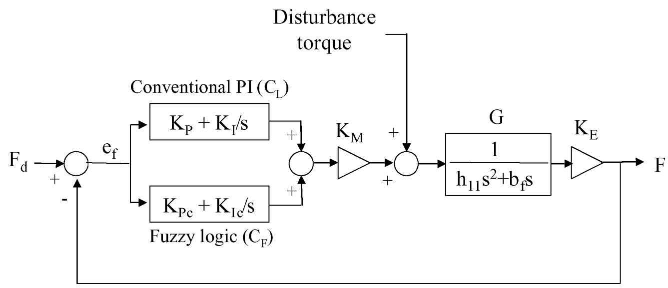

Fig. 4. Block diagram of the force control model. G represented the joint one of the robot and other symbols were explained in the text.

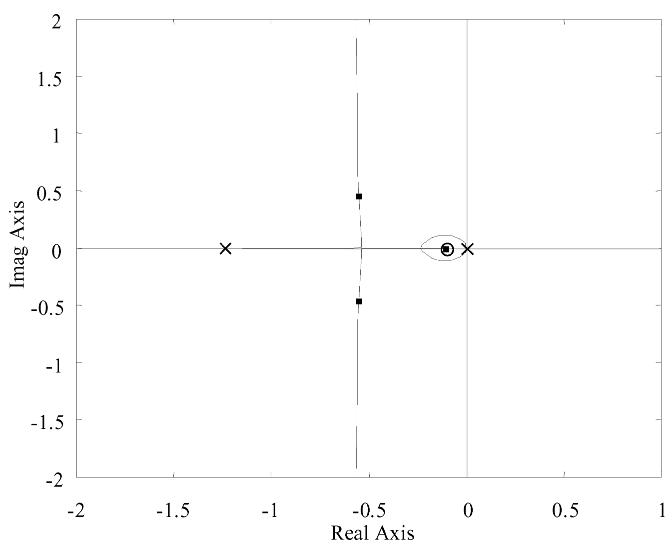

Fig. 5. Root locus plot of the one joint model of the robot. Solid squares showed the corresponding root loci of the system with the chosen control parameters.

D. Controller Stability Analyses

In order to analyze the stability of torque controller part, we employed both model simulation and conventional describing function analyses. From (3), one decoupled robot joint with the associated controller was modeled, as in Fig. 4. The transfer function of the decoupled robot joint 1 (G) could be expressed as

$$G = \frac{1}{h_{11}s^2 + b_f s} \tag{9}$$

where h_{11} and b_f were defined in (3) and (4). It was assumed that, during the robot movements, the robot links were in continuous movement and τ_c could be neglected. K_M was a constant. First, we worked on the controller without the fuzzy logic part. Since the contact stiffness (K_E) depended on the interaction with a subject, it was not a constant and could not be determined precisely. Accordingly, the optimal conventional PI controller parameters could not be determined. We set K_I/K_P as -0.1 and determined K_P empirically. Fig. 5 showed the effects of changing K_P, when K_E was assumed to be 1, on the system root loci. The system was stable as long as K_P was greater than zero. The thick dots showed the roots of the system at the chosen K_P that we used for the rest of this article. Then the fuzzy logic was added. The model was simulated by changing K_I and K_P and adding the fuzzy logic, as well as by adding Gaussian disturbance to excite the model. The Gaussian noises were used to represent all the disturbances, including the friction.

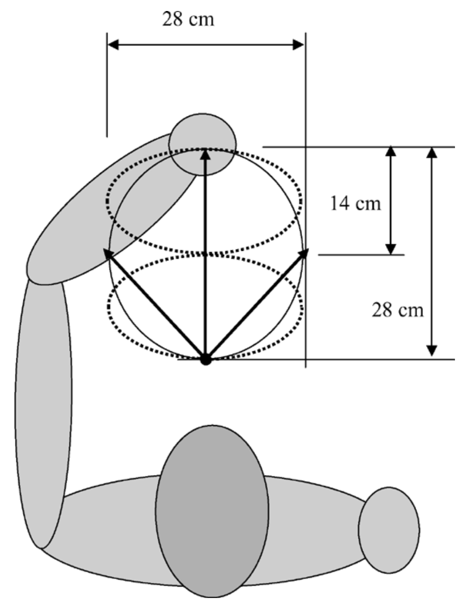

Fig. 6. Planned trajectories including linear, circular, and figure eight trajectories in both clockwise and counter-clockwise directions.

The stability of the model was also investigated by the conventional describing function analyses. According to Aracil and Gordillo [25], the describing function of the fuzzy force PI-controller could be defined as

$$[C_F(a,\omega) + C_L(a,\omega)] \cdot e_f(a,\omega) \tag{10}$$

where $e_f(a,\omega)$ was assumed to a simple sinusoidal function $a \cdot \sin(\omega t)$, both a and ω were constants, and

$$C_L(a,\omega) = K_P + \frac{K_I}{(a\cdot\omega)} \tag{11}$$

$$C_F(a,\omega) = \kappa 1 \cdot \mathrm{ssp}(a) + \frac{k2 \cdot \mathrm{ssi}\left(\frac{a}{\omega}\right)}{s} \tag{12}$$

$$\mathrm{ssp}(\ a) = \min\left[1, \frac{2}{\pi}\left(\sin^{-1}\frac{\mathrm{S_P}}{\mathrm{a}} + \frac{S_P}{a}\sqrt{1-\left(\frac{S_P}{a}\right)^2}\right)\right] \tag{13}$$

$$\mathrm{ssi}\left(\frac{a}{\omega}\right) = \min\left[1, \frac{2}{\pi}\left(\sin^{-1}\frac{S_I\cdot\omega}{a} + \frac{S_P\cdot\omega}{a}\sqrt{1-\left(\frac{S_P\cdot\omega}{a}\right)^2}\right)\right]. \tag{14}$$

S_I and S_P were the saturation limits of fuzzy logic for integration and proportional parts, respectively. As explained in the above, S_I and S_P were equal to K_I and K_P, respectively. The condition for the first harmonic balance was $1 + [C_F(a,\omega) + C_L(a,\omega)] \cdot G = 0$. The stability of the fuzzy controller was then visualized by drawing a series of curves of $[C_F(a,\omega) + C_L(a,\omega))]$ against $-G^{-1}$.

E. Trajectory Planning

We designed three types of movement trajectories, namely, linear, circular, and figure eight (Fig. 6). The normal linear

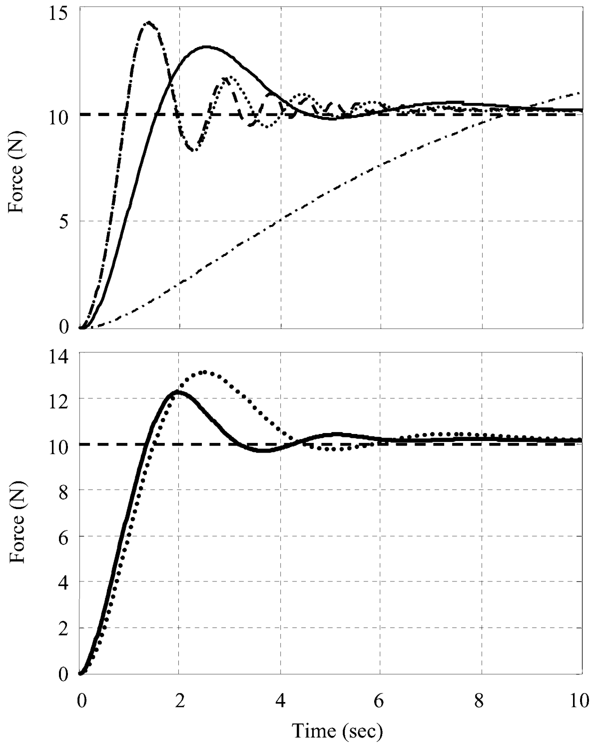

Fig. 7. Step responses of the simplified robot (G) with different control parameters. Upper plot showed the effects of changing K_P and K_I, where $K_P/K_I = 0.06/0/006$ (dashed–dotted line), 0.6/0/06 (solid line), 6/0.6 (dotted line) and 60/6 (dashed line), respectively. Lower plot demonstrated the effect of adding the fuzzy logic, with $K_P/K_I = 0.6/0/06$.

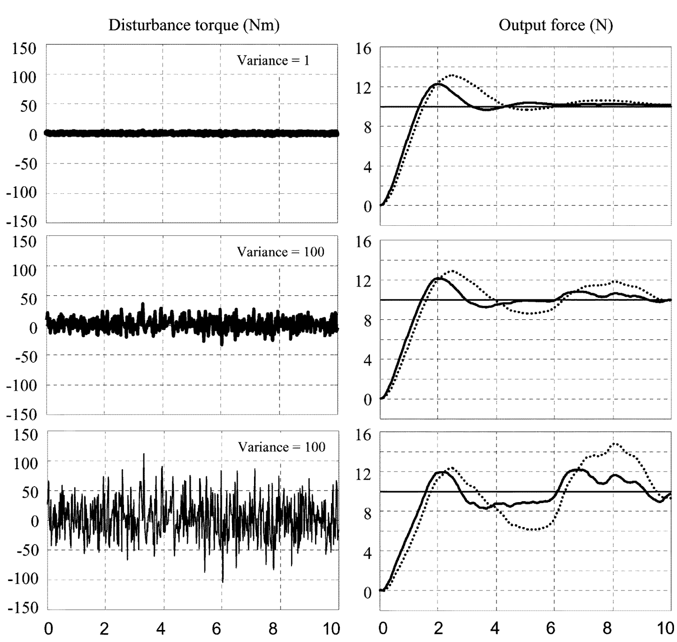

Fig. 8. Step responses of the controllers under different magnitudes of Gaussian disturbance. Solid lines: Classical PI controller plus the fuzzy logic. Dotted lines: Classical PI controller without the fuzzy logic.

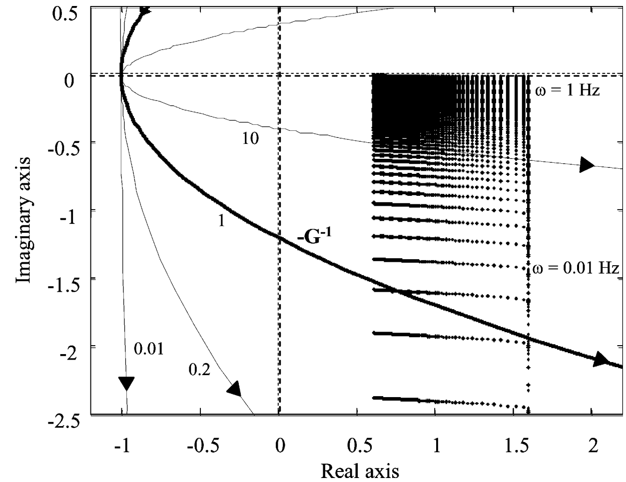

Fig. 9. Results of describing function analyses. Dots showed the trajectories of the controller due to the errors with frequencies ranging from 0.01 to 10 Hz and amplitudes from 0.1 to 100 N. Solid lines showed the trajectory of $-G^{-1}$ with different K_E values.

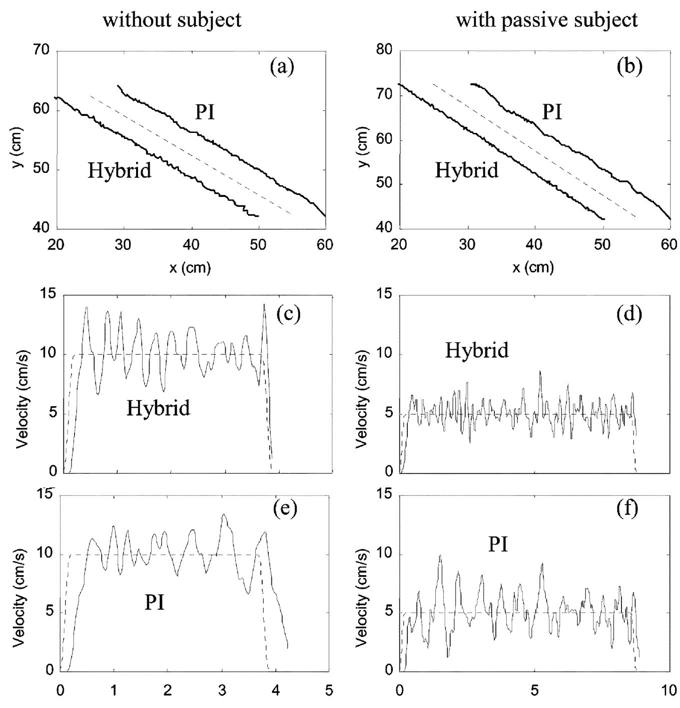

Fig. 10. Robot-alone without carrying a subject (left column) and passive (right column) linear movements of a normal subject. First row shows the movement trajectories. Upper solid line is shifted 5 cm to the right and the lower solid line is shifted 5 cm to the left for clarity. Dotted line is the target trajectory. Upper solid line represents the results with the conventional PI controller. Lower solid line represents the results using the hybrid fuzzy controller. Solid lines in the second and third rows are the corresponding velocity trajectories under hybrid fuzzy (second) and PI (third) controller respectively. Dotted line is the target velocity.

movement trajectory was an outward movement from the chest of 28 cm in length and the oblique linear movement trajectory was an oblique (45°) outward movement from the chest of 21.2 ($15 \cdot \sqrt{2}$) cm in length. The circular movement trajectory was a circular movement with a diameter of 28 cm. The figure eight movement trajectory consisted of two ellipses (14×28 cm) with their short axes in alignment in radial direction and with opposite moving directions. Since the movement velocity was not controlled, in the design process, a trajectory was partitioned into 4000 segments by length along the trajectory instead of the lapsed time [26].

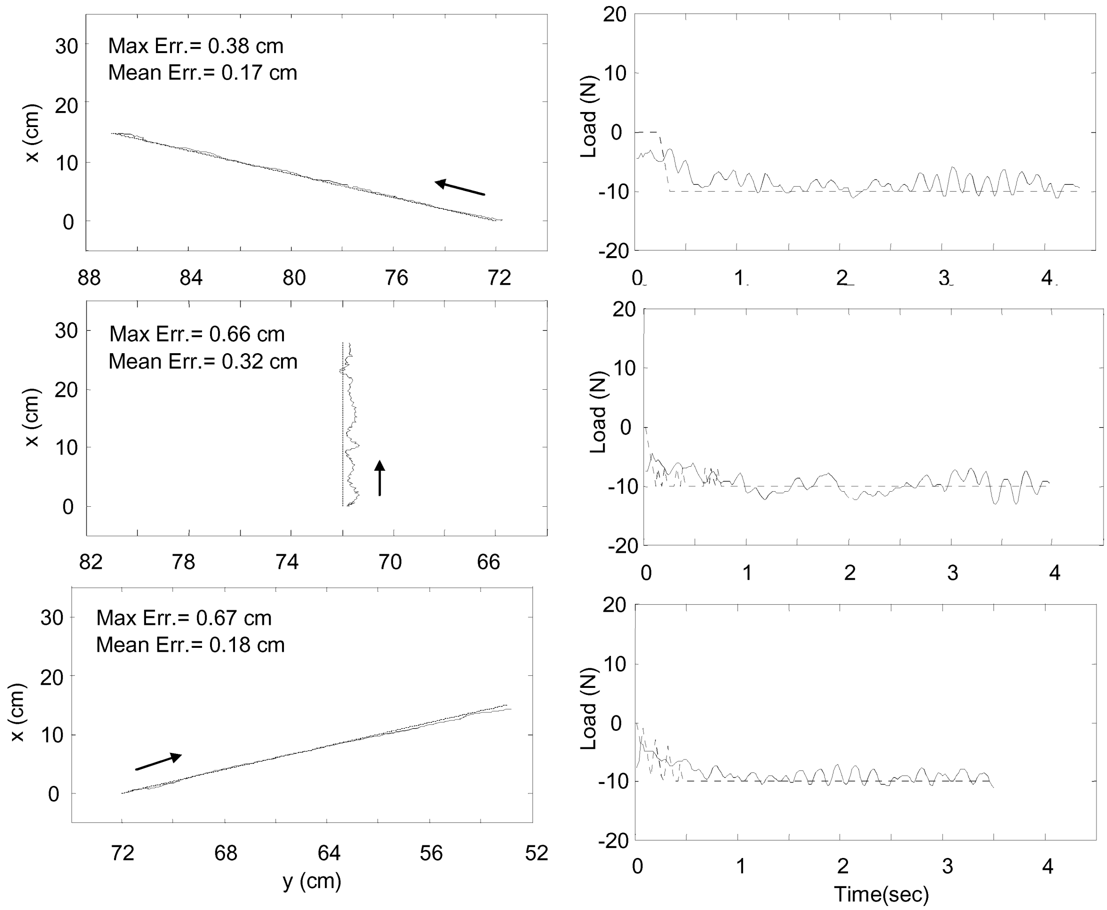

Fig. 11. Results of a normal subject performing active linear movements. Left column is the movement trajectories and the right column shows the force trajectories. Dotted lines are target paths and preset loads. Solid lines are actual trajectories and exerted forces.

F. Safety

Safety measures were implemented both in software and hardware levels. The robot stopped when the movement magnitude or velocity exceeded the predefined limits and the experimenter could stop the robot with an interruption command at any time. Four optical limit switches were employed to define the range of movement for both joints of the robot. The robot could also be stopped by shutting down the power supply with an emergency button by the patient or the physical therapist.

III. Results

A. Advantages and Stability of Fuzzy Force Control

Fig. 7(a) showed the simulated step responses of four sets of K_P and K_I for the conventional PI controller in the absence of fuzzy logic part. We chose $K_P = 0.6$ and $K_I = 0.06$ for the real robot. Fig. 7(b) demonstrated the contribution of the fuzzy logic. For the combination of K_P and K_I that we chose, the fuzzy logic made the response faster while reduced the magnitude of oscillation.

In addition, the fuzzy controller also contributed to the resistance to the external disturbance. Fig. 8 showed the step responses of the robot in face of Gaussian disturbances of different magnitudes. As the magnitude increased, the controllers became harder to keep a constant force level. The fuzzy logic helped to reduce the errors.

Fig. 9 showed the results of analyses by describing function method. The points in the right upper side of the solid curve ($-G^{-1}$) were the disturbances that did not jeopardize the system stability. The analyses showed that, with the implemented fuzzy controller, the robot arm was stable in face of disturbance of frequencies from 10 to 0.01 Hz and magnitudes from 0.1 to 100 N. In other words, the robot arm would be stable in the expected therapeutic maneuver ranges. The figure also showed that, as the contact stiffness (K_E) increased, the range of stability would be reduced.

B. Linear Passive and Active Movements

Fig. 10 showed the comparison of fuzzy and conventional PI controllers in robot-alone and passive left-oblique linear movements. Both the PI and the fuzzy controller could achieve the desired trajectory. The performance of the fuzzy controller was even better in both conditions. In the robot-alone condition, the means and standard deviations of the mean path errors for repeated trials were 0.148 ± 0.016 cm and 0.853 ± 0.096 cm, for the fuzzy and PI controllers, respectively. The difference was statistically significant by t-test ($p < 0.001$). On one normal subject in passive linear movements, the means and standard deviations of the mean path errors for repeated trials were 0.086 ± 0.021 cm and 1.014 ± 0.298 cm for the fuzzy and PI controllers

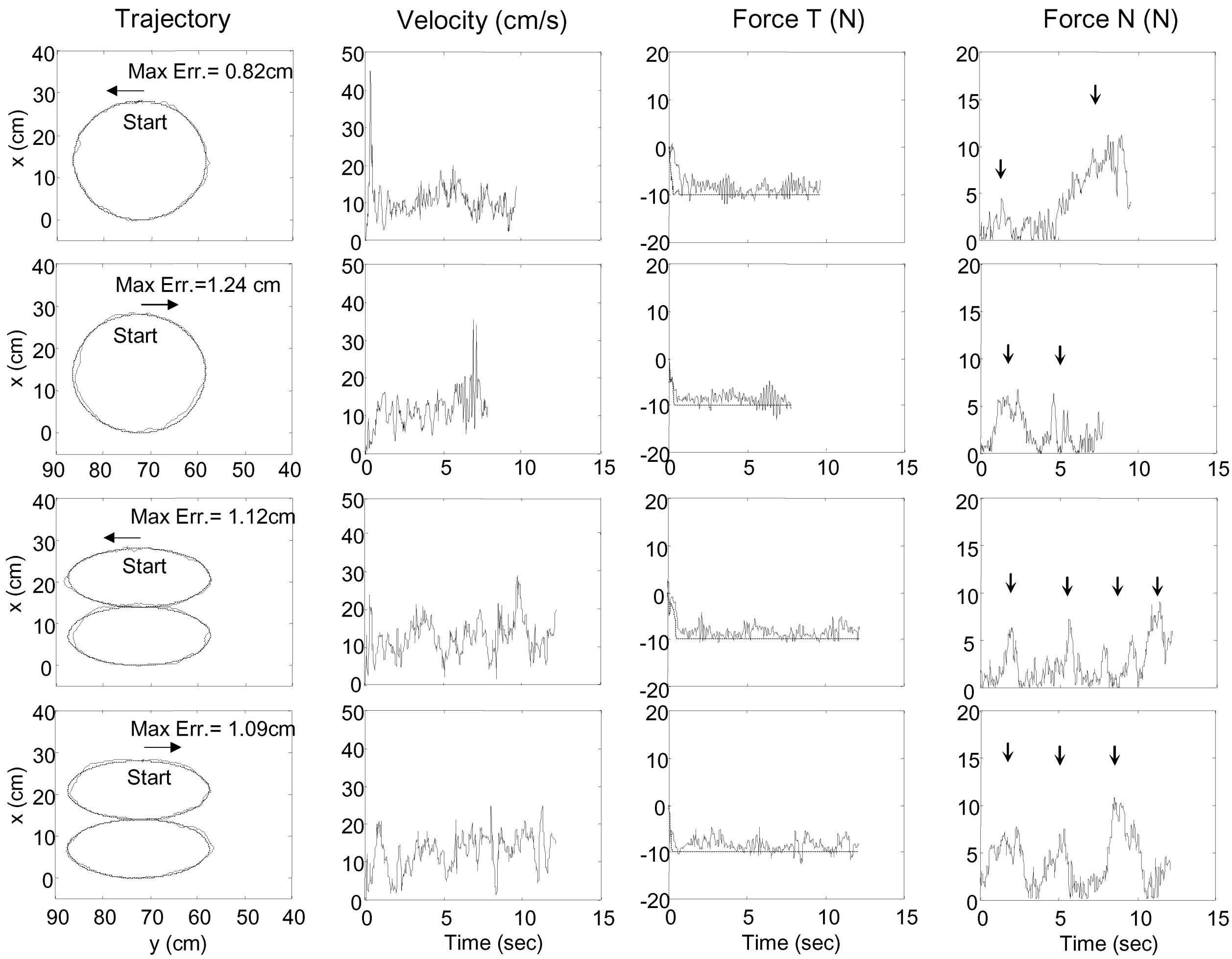

Fig. 12. Results of a normal subject performing circular and figure eight movements. First column (from left) shows the movement trajectories, the second velocity, the third the force in the tangential direction, and the fourth the absolute value of force in the orthogonal direction of the movement. Arrows in the first column indicate the direction of movement. Arrows in the fourth column mark the locations where the subjects need to change direction in the y axis.

respectively. The difference was also statistically significant by t-test ($p < 0.001$). The velocity profile derived from the fuzzy controller showed more frequent and smaller amplitude adjustments, in contrast to the coarser and less frequent adjustments in the case of conventional PI control. Though the adjustment seemed very busy, the movement of the robot was relatively smooth because of the natural damping effects of mechanical devices.

Fig. 11 showed the results of linear active movements of a normal subject against a load of ten Newtons along three directions. The robot with the fuzzy controller could guide the subject to perform the movement well in all three directions and, except at the beginning, kept the load constant as specified. On one normal subject moving the right upper limb, the means and standard deviations of the mean path errors for consecutive nine trials in left-oblique, straight-forward, and right-oblique directions were 0.432 ± 0.098 cm, 0.250 ± 0.029 cm, and 0.595 ± 0.122 cm, respectively.

C. Circular and Figure Eight Active Movements

Fig. 12 showed the results of circular and figure eight active movements of a normal subject against a load of ten Newtons. The trajectory was well maintained with the position error less than 1.25 cm during the whole trajectory in all four types of movements. Though the robot system did not regulate the moving velocity, we instructed the subject to keep the movement at constant velocity as possible by projecting the Cartesian coordinates against the desired movement on a monitor. The velocity profile showed that the velocity was relatively constant at 10 cm/s. The control system kept a resistive load of 10 N. In the fourth column, the force along the direction normal to the movement, showed that the subject could follow the trajectory well, except when the subject needed to change direction in the left-right axis (arrows).

IV. Discussion

There are several existing robot systems for rehabilitation, including MIT-MANUS [2], MIME [8], and reaching guide [5]. The basic construction principle of our robot and MIT-MANUS is similar. Impedance control, implemented in MIT-MANUS, is stable and robust to the uncertainties due to physical contact. Yet, the controller cannot control the position and force independently. When the preset impedance is small, subjects can more successfully complete movements at the expense of larger position errors. On the other hand, when the preset impedance is large, the position error is small but the subject is subjected to a larger off-trajectory resistance. The force/position hybrid control scheme developed in this work enables the robot to impose an assistive or resistive force to the subject, independent of the lateral position error. The fuzzy logic is intended to cope with the nonlinear dynamics of the robot mechanism and to ensure that the robot can operate for different subjects. The problem of our control scheme is that stability is difficult to prove or predict. We did many model analyses to compare the performance and stability of the fuzzy controller with the original PI controller that the fuzzy logic is added. The fuzzy controller is stable and has a faster response. MIME system is very flexible in programming and can be operated in two-side or one-side mode. While the two-side mode, working by position control, is similar to our robot in providing assistive force, the one-side mode in active-constrained mode is similar to our robot in providing resistive force. The other similar point is that both systems do not control velocity vigorously. The main difference is that our robot provides a constant force and MIME provides a viscous-like resistance. As in MIME system, our robot can also be programmed to operate in other operation modes but we have not fully explored these directions yet. Reaching guide has advantages in that the system is simpler and the hardware constraint is more solid. The disadvantage is that the trajectory is rigid and it may need different tracks for different treatment trajectories.

The applicability of our robot to the patient with spasticity is currently unknown. The robot will be safer as compared with the robots implemented with a pure position control. Stability of the force control part is a potential problem. A model of a human subject with spasticity is necessary for performing extensive simulations to test the stability of the man–robot system. Initially, we will choose patients with progressively more severe spasticity and observe the performance.

V. Conclusion

We designed an arm-like robot with hybrid position/force control scheme incorporating fuzzy logic. The controller was stable in the application range of movements and forces. The preliminary results using normal and stroke subjects showed that the robot successfully guided the subject through linear and circular movements. The robot could also impose a constant force on the subject during the movement. The next step is to evaluate the effectiveness of this robot in assisting patients in a larger scale rehabilitation program.

References

[1] T. Noritsugu and T. Tanaka, "Application of rubber artificial muscle manipulator as a rehabilitation robot," *IEEE/ASME Trans. Mechatronics*, vol. 2, no. 4, pp. 259–267, Dec. 1997.

[2] H. I. Krebs, N. Hogan, M. L. Aisen, and B. T. Volpe, "Robot-aided neurorehabilitation," *IEEE Trans. Rehab. Eng.*, vol. 6, no. 1, pp. 75–87, Mar. 1998.

[3] M.-S. Ju, C.-C. K. Lin, J.-R. Chen, H.-S. Cheng, and C.-W. Lin, "Performance of elbow tracking under constant torque disturbance in stroke patients and normal subjects," *Clinical Biomech.*, vol. 17, pp. 640–649, 2002.

[4] J. A. Cozens, "Robotic assistance of an active upper limb exercise in neurological impaired patients," *IEEE Tran. Rehab. Eng.*, vol. 7, no. 4, pp. 254–256, Jun. 1999.

[5] D. Reinkensmeyer, C. Takahashi, and W. Timoszyk, "Evaluation of an assistive controller for reaching following brain injury," in *Proc. 1st Joint BMES/EMBS Conf.*, 1999, p. 631.

[6] M. H. Raibert and J. J. Craig, "Hybrid position/force control of manipulators," *Trans. ASME J. Dyn. Syst., Meas. Control*, vol. 102, pp. 126–133, 1981.

[7] H. Suh, J. H. Hong, S.-R. Oh, and K. B. Kim, "Fuzzy rule based position/force control of industrial manipulators," in *Proc. IEEE/RSJ Int. Workshop Intelligent Robots Syst.*, vol. 3, Nov. 3–5, 1991, pp. 1617–1622.

[8] P. S. Lum, C. G. Burgar, P. C. Shor, M. Majmundar, and H. F. M. Van der Loos, "Robot-assisted movement training compared with conventional therapy techniques for the rehabilitation of upper-limb motor function after stroke," *Arch. Phys. Med. Rehab.*, vol. 83, no. 7, pp. 952–959, 2002.

[9] C. G. Burgar, P. S. Lum, P. Shor, and H. F. M. Van der Loos, "Development of robots for rehabilitation therapy: The Palo Alto VA/Standord experience," *J. Rehabil. Res. Develop.*, vol. 37, no. 6, pp. 663–673, 2000.

[10] L.-X. Wang, *Adaptive Fuzzy Systems and Control: Design and Stability Analysis*. Englewood Cliffs, NJ: Prentice Hall, 1994.

[11] W. J. Rugh, "Analytical framework for gain scheduling," *IEEE Control Syst. Mag.*, pp. 79–84, 1991.

[12] S. H. Lee, S. G. Kim, and J. T. Lim, "Fuzzy-logic-based fast gain-scheduling control for nonlinear suspension systems," *IEEE Trans. Ind. Electron.*, vol. 45, no. 6, pp. 953–955, Dec. 1998.

[13] K. Tanaka and H. O. Wang, *Fuzzy Control Systems Design and Analysis*. New York: Wiley, 2001.

[14] A.-A. S. Ibrahim, "Nonlinear PID controller design using fuzzy logic," in *IEEE MELECON 2002*, Cairo, Egypt, May 7–9, 2002.

[15] U.-C. Moon and K. Y. Lee, "Hybrid algorithm with fuzzy system and conventional PI control for the temperature control of TV glass furnace," *IEEE Trans. Control Syst. Technol.*, vol. 11, no. 4, pp. 548–554, Jul. 2003.

[16] J. Deskur, R. Muszynski, and D. Sarnowski, "Tuning and investigation of combined fuzzy controller," in *Proc. 7th Int. Conf. Power Electron. Variable Speed Drives*, Sep. 21–23, 1998.

[17] M. S. Ju, S. H. Yi, Y. G. Tsuei, and Y. L. Chou, "Fuzzy control of electrohydraulic above-knee prostheses," *JSME Int. J.*, ser. C, vol. 38, pp. 78–86, 1995.

[18] M. S. Ju and D. L. Yang, "Design of adaptive fuzzy controls based on natural control laws," *Fuzzy Sets Syst.*, vol. 81, pp. 191–204, 1995.

[19] J. J. J. Chen, Y. N. Yu, D. G. Hung, B. T. Ann, and G. C. Chang, "Applying fuzzy logic to control of cycling movement induced by functional electrical stimulation," *IEEE Trans. Rehabil. Eng.*, vol. 5, pp. 158–169, 1997.

[20] H. Asada and K. Youcef-Toumi, "Analysis and design of a direct-drive arm with a five- bar-link parallel drive mechanism," *Trans. ASME J. Dyn. Syst. Meas. Control*, vol. 106, pp. 255–230, Sep. 1984.

[21] S. M. Phillips and K. R. Ballou, "Friction modeling and compensation for an industrial robot," *J. Robot Syst.*, vol. 10, pp. 947–971, 1993.

[22] Z. Lu, K. B. Shimoga, and A. A. Goldenberg, "Experimental determination of dynamic parameters of robotic arms," *J. Robot Syst.*, vol. 10, pp. 1009–1029, 1993.

[23] C. C. Lee, "Fuzzy logic in control systems: Fuzzy logic controller—Part 1," *IEEE Trans Syst. Man Cybern.*, vol. 20, no. 2, pp. 402–417, Mar./Apr. 1990.

[24] Z. Y. Chou, "Contact force control in soft boundary condition," M.S. thesis (in Chinese), Nat. Yung-Lin Technol. College, Dept. Mech. Eng. Technol., Toliu, Taiwan, 1997.

[25] J. Aracil and F. Gordillo, "Describing function method for stability analysis of PD and PI fuzzy controllers," *Fuzzy Sets Syst.*, vol. 143, pp. 233–249, 2004.

[26] T. Yoshikawa, *Foundations of Robotics: Analysis and Control*. Cambridge, MA: MIT Press, 1990.

Ming-Shaung Ju was born in 1956. He received the B.Sc. and M.Sc. degrees in mechanical engineering from National Cheng Kung University (NCKU), Tainan, Taiwan, R.O.C., in 1978 and 1982, respectively, and the Ph.D. degree in mechanical engineering from Case Western Reserve University, Cleveland, OH, in 1986.

In 1987, he joined the Faculty of Mechanical Engineering Department, NCKU, where he was an Associate Professor and became a Professor in 1993. He has worked in biomechanics, biocybernetics, mechatronics, and microelectromechanical systems for biomedical engineering applications. He has served on many scientific committee boards in Taiwan, namely, the Chinese Society of Mechanical Engineering, the Chinese Society of Biomedical Engineering and the Formosa Society of Biomechanics. He is also a member of the Man–Machine System Committee of the International Federation for the Theory of Machines and Mechanisms.

Chou-Ching K. Lin received the B.S. degree in medicine from National Yang-Ming University, Taipei, Taiwan, R.O.C., in 1988, and the M.Sc. and Ph.D. degrees in biomedical engineering from Case Western Reserve University, Cleveland, OH, in 1994 and 1997, respectively.

Since passing the Taiwan Neurology and Gerontology Boards in 1999 and 2003, he joined the Department of Neurology, Medical Center, National Cheng Kung University, Tainan, Taiwan, R.O.C., as a Clinical Assistant Professor. His areas of interest include functional electrical stimulation, neuro-rehabilitation, neural electrophysiology, and nerve regeneration.

Dong-Huang Lin was born in 1974. He received the B.Sc. degree in mechanical engineering from National Central University, Taipei, Taiwan, R.O.C., in 1997, and the M.Sc. degree in mechanical engineering from National Cheng Kung University, Tainan, Taiwan, R.O.C., in 2001.

He has been worked on robotics for rehabilitation engineering applications.

Ing-Shiou Hwang received the B.S. degree in physical therapy from National Taiwan University, Taipei, Taiwan, R.O.C., in 1988, the M.S. degree in biomedical engineering from National Cheng Kung University, Tainan, Taiwan, R.O.C., in 1993, and the Ph.D. degree in biomedical engineering from the University of Texas, Austin, in 1998.

In 1999, he was with the School of Physical Therapy, National Cheng Kung University as an Assistant Professor. He was also an Executive Editor of the *Formosan Journal of Physical Therapy*, official journal of the Physical Therapy Association of the R.O.C. (Taiwan), from 1999 to 2001. Since 2002, he has been an Associate Professor in the Department of Rehabilitation, National Cheng Kung University. His major research interests are in biosignal processing, clinical electrophysiology, and rehabilitative neuroscience.

Shu-Min Chen received the M.D. degree from the Department of Medicine, National Cheng Kung University (NCKU), Tainan, Taiwan, R.O.C., in 1992.

She has served in the Department of Physical Medicine and Rehabilitation, Medical Center, NCKU since 1992. She has more than 10 years of clinic experience in the field of rehabilitation. In 1995, she served on the National Board of the Rehabilitation Medicine Association, Taiwan. She has been an Assistant Professor of Physical Medicine and Rehabilitation, Medical Center, NCKU, since 2002. Her major interests include myofascial pain syndrome, neuromuscular rehabilitation, and musculoskeletal sonography.